VERA RUBIN RIDGE (GALE CRATER, MARS) GRAIN SIZE OBSERVATIONS FROM CHEMCAM LIBS DATA, AND INTERPRETATIONS

F. Rivera-Hernandez[1], D. Y. Sumner[2], N. Mangold[3], K. M. Stack[4], K. S. Edgett[5], K. A. Bennett[6], R. C. Wiens[7], V. Z. Sun[4], E. Heydari[8], S. Maurice[9], [1]Dartmouth College, Earth Sciences, Hinman Box 6105, Hanover, NH, 03755 (frances.rivera-hernandez@dartmouth.edu); [2] UC Davis, CA; [3] Université de Nantes, LPGN, France; [4]Jet Propulsion Laboratory, CA; [5]Malin Space Science Systems, CA; [6]USGS Astrogeology Science Center, AZ; [7]Los Alamos National Lab, NM; [8] Jackson State University, MS; [9]IRAP, U. Toulouse, CNRS, UPS, CNES, France

Introduction: Since Sol ~1800, the *Curiosity* rover has been exploring Vera Rubin Ridge (VRR), a linear topographic feature that parallels the northern perimeter of lower Aeolis Mons (informally, Mt. Sharp) in Gale crater, Mars [Fig. 1, 1]. In data acquired from orbiting spacecraft, the VRR is distinct from the sub- and superjacent rocks due to its erosional resistance (Fig. 1) and strong hematite spectral signature [2]. However, from rover images, there does not appear to be a stratigraphic facies change from the underlying Murray formation (dominated by laminated mudstones) to the VRR [2, 3]. This continuity in mudstone facies suggests that the VRR rocks are also part of the Murray formation and were also likely deposited in a lake [2, 3]. The reason for the erosion resistance and morphology of the VRR ridge is still unknown [2]. However, it is possible that there are grain size variations or cement in VRR rocks that have not been detected by images or where not sampled by the rover [2].

To supplement knowledge of grain sizes gained from examination of image data, this study uses ChemCam Laser Induced Breakdown Spectroscopy (LIBS) data and the Gini Index Mean Score (GIMS) [4] to infer grain sizes in VRR rocks. Results from this study provide further insights into grain size and facies changes preserved in the Murray formation through the VRR to Sol 2150.

Methods: Grain-sizes can be inferred from the GIMS, a composition-based grain-size proxy that uses point-to-point chemical variabilities in major-element oxide compositions in ChemCam LIBS data [4]. The diameter of each point vaporized by the ChemCam laser ranges between 0.4-0.6 mm [medium to coarse sand in size; 5, 6]. Thus, rocks with grains smaller than the laser spot size (e.g., mudstones), produce bulk rock compositions at all LIBS points and low point-to-point chemical variability [4, 7-11]. In contrast, those with grains about the size of the spot or larger (e.g., sandstones) provide contributions from individual grains at each point and often have high point-to-point chemical variability. The presence of sand can be inferred for coarse rocks with non-uniform compositions and grains smaller than 2 mm in size [very fine gravel; 4].

The GIMS was used to quantify the chemical variability in the ChemCam LIBS data by averaging the Gini Index of seven normalized major-element oxides [4]. The Gini index is a non-dimensional statistical parameter that varies from 0 to 1 [12]. The output of the GIMS is a mean Gini index, G_{MEAN}, and a standard deviation, STDr, for each LIBS observation [4]. Finer-grained rocks have smaller G_{MEAN} than coarser-grained rocks [4]. Textural analyses from images taken by the Mars Hand Lens Imager (MAHLI), and the ChemCam Remote Micro Imager (RMI) were used to exclude targets with resolvable diagenetic features from the GIMS analysis.

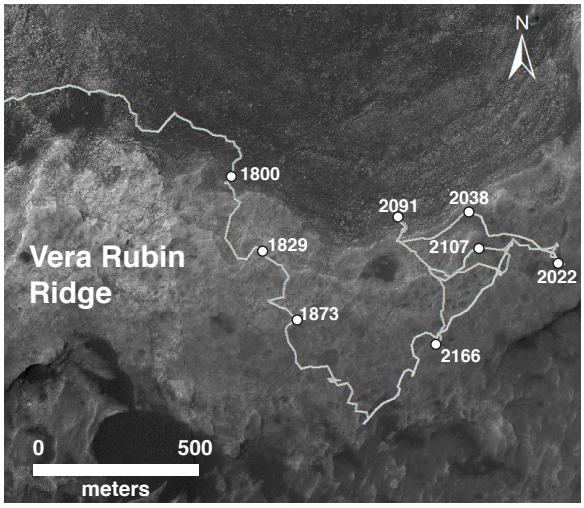

Figure 1. HiRISE mosaic of the Vera Rubin Ridge with the *Curiosity* rover traverse up to sol 2166.

The GIMS was first applied to rocks of known grain size in the Murray formation to develop a G_{MEAN} grain size scale [4, 13]. Four grain size regimes were defined for the Murray formation based on correlations between the Wentworth scale and G_{MEAN}: mud (G_{MEAN}=0.00-0.07), silt to fine sand (G_{MEAN}=0.07-0.10), fine to medium sand (G_{MEAN}=0.11-0.16), and medium to coarse sand (G_{MEAN}=0.17-0.34). These grain size regimes were used to predict the particle size of rocks of unknown grain size encountered along Curiosity's traverse in the rest of the Murray formation, including the VRR.

Results: Preliminary results using the GIMS on 155 rocks suggest that the VRR is dominated by mudstones with grain sizes below the spatial resolution capabilities of all *Curiosity* cameras (Fig. 2). Intervals of fine to medium sandstones were also detected. The grain size of most fine sandstones identified by GIMS could not be verified due to an absence of sufficiently high-resolution images. However, several predicted fine sandstones from the

Table 1. Statistics for grey and red Jura rocks that are associated with MAHLI images.

Jura color	# of rocks	Mean G_{MEAN}	Mean grain size bin	Standard Deviation
Red	16	0.05	mud	0.03
Grey	10	0.09	silt to fine sand	0.03

Jura member have granular textures suggesting that grains coarser than mud may be present.

Jura member rocks with granular textures are predominantly grey in color and these are distinct from other rocks in the Jura and the rest of the VRR which are red in color. The grey Jura rocks have a mean G_{MEAN} of 0.09, which falls in the silt to fine sand grain size bin (Table 1). Instead, red Jura rocks have a lower mean G_{MEAN} of 0.05, which is the mud grain size bin (Table 1).

Interpretations and Discussion: From rover image data, the Mars Science Laboratory team divided the upper Murray formation into three members: Blunts Point, Pettegrove Point, and Jura. From orbital mapping, the Pettegrove Point and Jura members correspond to the geomorphic expression of the VRR (i.e, the top of the ridge). Here we discuss results for all three members.

In the Blunts Point member, sandstones are absent in the GIMS analysis and in MAHLI images. The dominance of mudstone accumulation is consistent with a lacustrine depositional environment. This is in contrast to the underlying rocks of the upper Sutton Island member, for which the GIMS analysis shows the rocks are dominated by medium to coarse sandstones (Fig. 2), suggesting deposition in a fast flow, either an aeolian or fluvial environment. This facies transition from Sutton Island into the Blunts Point member suggests a depositional change from a subaerial environment to a subaqueous environment.

Above Blunts Point on the VRR, the facies in the Pettegrove Point and the Jura members are mixed, containing mostly mudstones with intervals of very fine sand sandstones. The sandstone suggests deposition from bedload transport in medium speed flows, consistent with nearshore lacustrine or floodplain environments.

Within the Jura, small variations in G_{MEAN} between grey and red colored rocks may represent subtle changes in mean grain size. If so, the grey Jura rocks are generally coarser-grained than those that are red in color (Table 1; Fig. 2). However, the majority of the VRR rocks are similar in grain size to those underlying them in the rest of the Murray formation (Sutton Island and lower). In contrast, diagenetic features are more abundant in the VRR, including concretions [14, 15], veins [15], elongate iron-rich features, sand-sized lenticular shaped features, and others [15]. The relationships between diagenetic features and the GIMS are still being investigated.

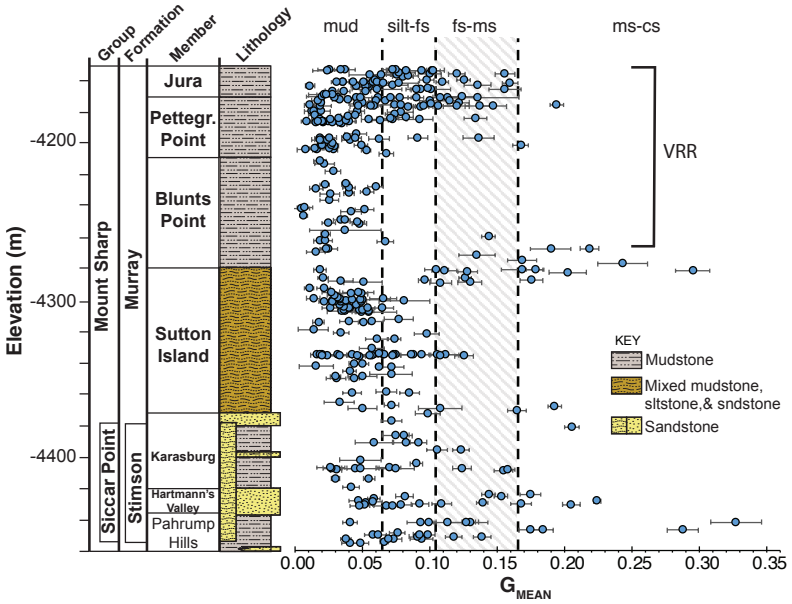

Figure 2. Elevation versus G_{MEAN} for rocks used in the GIMS analysis plotted with the stratigraphic column of the Murray formation on the left. Grain sizes ranges are over plotted on the graph: clay to silt (mud), silt to fine sand (fs), fine to medium sand (fs-ms), and medium to coarse sand (ms-cs). The hashed pattern for the fs-ms bin means that the bounds are not well constrained.

References: [1] Heydari et al. (2018) LPSC 49 Abstract #1817. [2] Fraeman et al. (2018) LPSC 49 Abstrac t #1557 [3] Edgar et al. (2018) LPSC 49 Abstract #1704 [4] Rivera-Hernandez et al. (2019) *Icarus*. doi: 10.1016/j.icarus.2018.10.023 [5] Maurice et al. (2012). *Space science reviews*, 170(1-4), 95-166 [6] Wiens et al. (2012) *Space Science Reviews*, *170*(1-4), pp.167-227. [7] Anderson et al. (2011). *Icarus*, *215*(2), pp.608-627. [8] McCanta et al. (2013) *Planetary and Space Science*, *81*, 48-54. [9] Sivakumar et al. (2014) *Spectrochimica Acta Part B: Atomic Spectroscopy*, *92*, 84-89. [10] Mangold et al. (2017) *Icarus*, *284*, 1-17. [11] McCanta et al. (2017) *GSA Today*, *27*(7). [12] Gini (1921) *The Economic Journal*, *31*(121), pp.124-126. [13] Rivera-Hernandez et al. (2018) LPSC Abstract #2973 [14] Sun et al. (in press) Icarus. doi:10.1016/j.icarus.2018.12.030. [15] L'Haridon et al. LPSC 50 (this volume)